

SUPPLEMENTAL INFORMATION – Transgenic mice expressing caspase-6 derived N-terminal fragments of mutant huntingtin develop neurologic abnormalities with predominant cytoplasmic inclusion pathology composed largely of a smaller proteolytic derivative

Supplemental Video 1. N586-82Q-C63 mice exhibit dyskinesia and ataxia. Mice were video recorded once a week (Sony Camera DSC-P31, Tokyo, Japan) to observe the progressive ataxic phenotype. Video representative of the dyskinesia/ataxia was assembled on Windows Movie Maker (Microsoft, Redmond, WA).

Supplemental Video 2. N586-23Q-A2 mice show no obvious movement abnormalities. Ten-month old mice were videotaped as described above.

Supplemental Video 3. N586-82Q-C62 mice exhibit dyskinesia and ataxia. Fifteen month old line 62 mice demonstrate near identical motor phenotypes to line C63 mice.

Supplemental Figure S1. Northern blot analysis of N586-82Q transgene expression. The level of transgene mRNA in the mice from Line 63 was estimated to be about 2 fold higher than that of Line 62. Note that in both cases, the levels of mutant htt mRNA in brain of N586-82Q mice were lower than the previously generated HD-N171-82Q line 81 mice. Non-transgenic mice (NTg). The bottom panel shows 28S rRNA as a loading control.

Methods: Total mouse brain RNA was isolated using the TRIzol reagent (Invitrogen, Carlsbad, CA). Five µg of total RNA was separated through a formaldehyde/agarose gel and transferred to a Genescreen Plus membrane (PerkinElmer, Boston, MA). The membrane was then incubated with radiolabeled probe (Ready-To-Go DNA Labeling Beads (-dCTP), GE Amersham, Piscataway, NJ) using the htt DNA sequence coding for amino acids 80-171 as the template.

Supplemental Figure S2. Immunoblot analysis of mice expressing N586-82Q and N586-23Q. The levels of transgene expression in forebrain homogenates of N586-82Q-

C63 and N586-23Q-A2 mice were compared by immunoblot with htt antibody 2B4. Homogenates from 3 individual animals were compared (50µg protein per lane). HEK293 cells transfected (293 Tfx) with cDNAs encoding htt were also used as controls (15µg protein per lane). The blot was re-probed with antibodies to SOD1 (m/h SOD1 antibody) to assess loading. Arrowheads identify full-length N586-23Q protein and arrowheads identify full-length N586-82Q protein.

Methods: The methods used in preparing brain tissues for immunoblot analyses are described in the main text. For cell transfection studies, HEK293 cells were transfected with Lipofectamine 2000 (Invitrogen) at ~80% confluence with pcDNA3.1(+) expression vectors encoding htt cDNAs. The transfection reaction was replaced with normal media (DMEM + 10% horse serum) after 24h and cells were harvested after another 24h. Cell pellets were sonicated in PBS + protease inhibitor cocktail (Sigma P8340) followed by a brief centrifugation and colorimetric BCA protein concentration assay (Pierce, Rockford, IL).

Supplemental Figure S3. The CA1 and CA3 regions of hippocampus in N586-82Q-C63 mice shows profound degeneration. Hematoxylin and eosin staining highlighted the loss of the CA1 and CA2 regions of the hippocampus. Partial degeneration of the CA3 region was also noted. By contrast, the hippocampus of N586-23Q-A2 mice appeared to have normal architecture.

Supplemental Figure S4. Most regions of the brain show inclusion pathology in N586-82Q-C63 mice. A composite image of immunofluorescent staining of a symptomatic N586-82Q-C63 animal is shown. Almost most all immunoreactivity for the N586-82Q protein is concentrated in inclusions (see Figs. 6, 7, and 10 of main text) and thus all red staining is indicative of the presence of inclusions.

Supplemental Figure S5. The cortex and hippocampus harbor numerous htt inclusions. Immunohistochemical visualization of cortex and hippocampus of symptomatic N586-82Q-C63 mice by immunostaining with the htt antibody 2B4 developed with secondary antibodies coupled to horse-radish peroxidase and DAB. Large

extranuclear inclusions were seen (A). By contrast, cortex from line A2 (B) or NTg littermates (C) did not show htt inclusions. Similar inclusion pathology was seen in the hippocampus of N586-82Q-C63 mice (D,G,J) but not the N586-23Q-A2 mice (E,H,K) or NTg mice (F,I,L).

Supplemental Figure S6. Cytoplasmic inclusions occur in both lines of N586-82Q mice, and these inclusions are larger than the inclusions of HD-N171-82Q line 81 mice. A and B) Staining of cerebellum and cortex, respectively, of symptomatic N586-82Q-C63 mice with the 2B4 antibody (red), revealed large, cytoplasmic aggregates. Similar results were seen in cerebellum and cortex of line C62 mice (15 m/o) (C and D, respectively). Compared to N586-82Q mice, the same brain regions of N171-82Q line 81 mice exhibited small inclusions (E and F, respectively). Dashed white lines were added to delineate nuclear boundaries in the N171-82Q sections because the intensity of the DAPI fluorescence obscures that htt inclusion when visualized under conditions that reveal the complete boundary of the nucleus.

Supplemental Figure S7. Progressive accumulation of htt inclusions and progressive degeneration of cerebellar granule cells in N586-82Q-C63 mice.

Row A) In NTg cerebellum, immunostaining with the 2B4 antibody (amino acids 59-65) was diffuse and the granule cell layer, as visualized by nuclear staining with DAPI, was densely packed and normal in appearance. By contrast, in 2 month old mice from line C63 we largely observed punctate immunoreactivity for htt (Row B). At this age, the granule cell layer was still densely packed with neurons and normal in appearance (middle). Row C) In 8 month old N586-82Q-C63 mice that were severely ataxic, we observed large htt immunoreactive inclusions throughout the granule cell layer with obvious thinning and degeneration of the granule cell layer.

Supplemental Figure S8. Cortical and cerebellar inclusions in HD-586-82Q-eGFP mice are detected by Thioflavin S. A and B) Images of cerebellum and striatum from a symptomatic N586-82Q-C63 animal stained with Thioflavin S. Note that the staining procedure includes pretreatments with 0.25% potassium permanganate solution for 5

minutes followed by 1% potassium metabisulfate/1% oxalic acid solution for 5 minutes; these treatments destroy the inherent fluorescence of eGFP. Thus the fluorescence seen in these images derives specifically from Thioflavin S fluorescence. C and D) Images from cerebellum of 8 month old N586-23Q-A2 mice. E and F) Images from age-matched nontransgenic littermates of N586-82Q-C63 mice. These images are representative of what was visualized in 3 different symptomatic animals on at least 3 tissue sections from each animal.

Methods: Thioflavin S staining was performed according to the Guntern standard protocol with small modifications (1). Briefly, sections stored in anti-freeze solution were washed by PBS, and then mounted to slides and dried completely. The slides were immersed in 0.25% potassium permanganate solution for 5 minutes, then 1% potassium metabisulfate/1% oxalic acid solution for 5 minutes, and then 0.02% Thioflavin-S solution (Chroma-Gesellschaft, Schmid, Kongen, Germany) for 10 min. Excess dye was removed by brief rinses in 70% ethanol, then in water, after which slides were finished in aqueous mounting medium for fluorescent microscopy.

Supplemental Figure S9. Line C63 mice exhibit astrogliosis. Increased GFAP immunoreactivity was obvious in striatum, cortex, cerebellum, and hippocampus in the N586-82Q-C63 mice as compared to N586-23Q-A2 or NTg mice. These images are representative of what was visualized in 3 different symptomatic animals on at least 3 tissue sections from each animal.

Supplemental Figure S10. Htt aggregates are not found within the cell bodies of astroglia. A) Very little immunoreactivity was observed in NTg mouse brain sections immunostained with the htt antibody 2B4 (red) and GFAP (green). In contrast, line C63 cortex (B and D, low and high magnification, respectively) and striatum (C) exhibited astrogliosis in regions rich with htt aggregates. However, there was no direct co-localization of htt and GFAP in cell bodies. DNA is stained blue with DAPI.

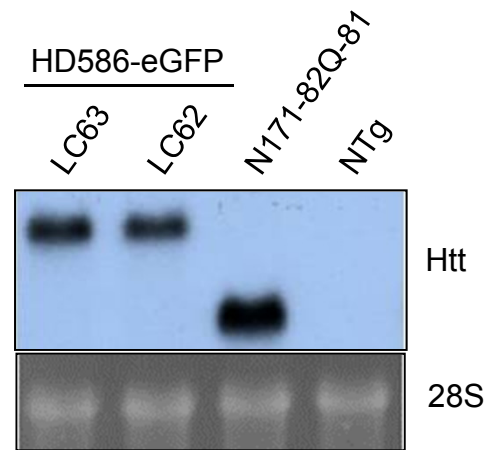
Supplemental Figure S11. Inclusions in line C63 mice contain the entire N586-82Q protein. Row A) We co-immunostained line C63 mouse brains with a peptide antibody for htt residues 64-82 (red) and with 1H6 (green). The merged image of these antibodies shows that all aggregates appear yellow suggesting co-localization. Row B) We also co-immunostained using htt antibodies htt64-82 (red) and 2166 (green) and again find that after merging images, all aggregates appear yellow. These data indicate that all inclusions contain some full-length N586-82Q protein.

Supplemental Figure S12. GFP is soluble and does not co-localize with htt aggregates. The cortex and cerebellum of symptomatic N586-82Q-C63 and NTg littermates was homogenized and fractionated by centrifugation in buffers containing NP40 into soluble and insoluble fractions (see Methods of main text). Each fraction was then analyzed by immunoblot with antibodies to GFP. This blot was originally probed with htt antibody 2B4; faint high molecular weight htt bands are seen in lanes 3 and 4. All detectable GFP migrated at the expected size and was soluble in detergent. This outcome was consistent with histologic analyses in which GFP did not show obvious co-localization with htt inclusions.

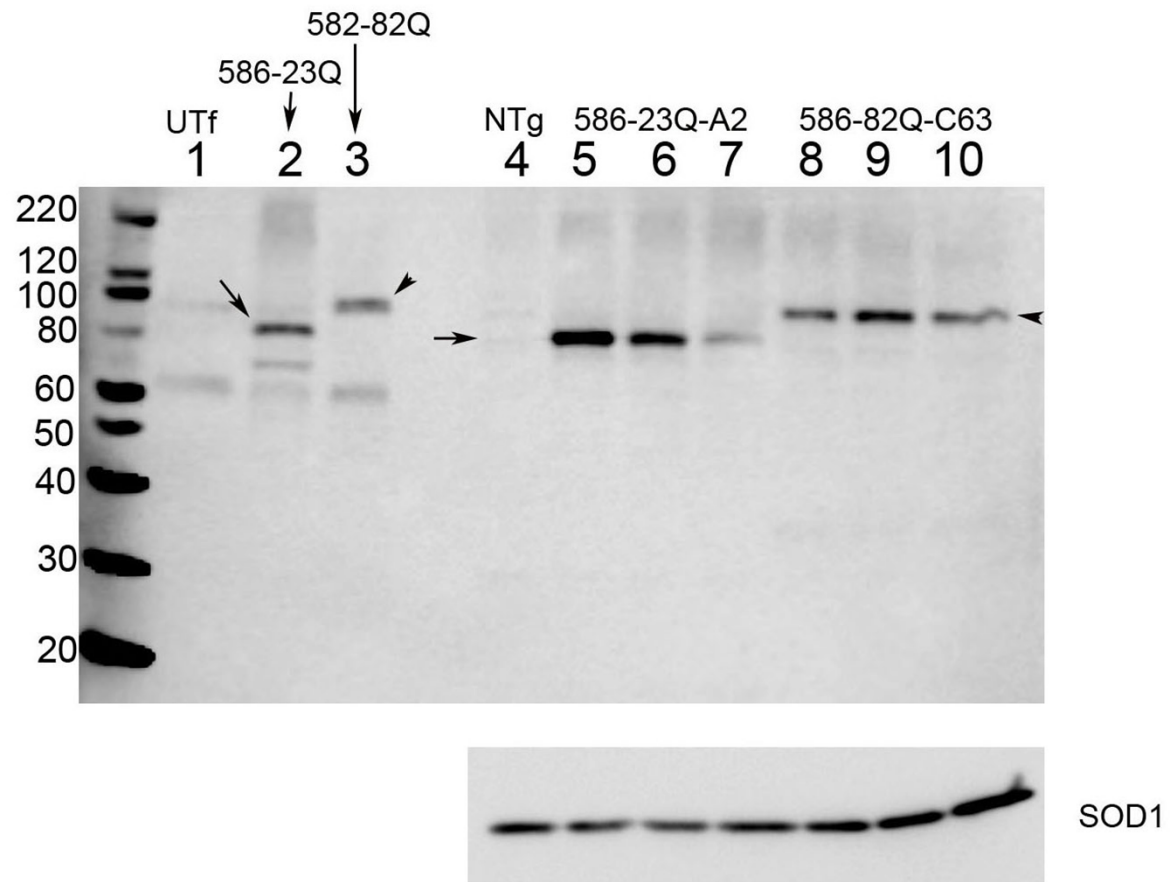
References

1. Jankowsky, J.L., Slunt, H.H., Gonzales, V., Savonenko, A.V., Wen, J.C., Jenkins, N.A., Copeland, N.G., Younkin, L.H., Lester, H.A., Younkin, S.G. et al. (2005) Persistent amyloidosis following suppression of Abeta production in a transgenic model of Alzheimer disease. *PLoS. Med.*, **2**, e355-

Suppl. Fig S1

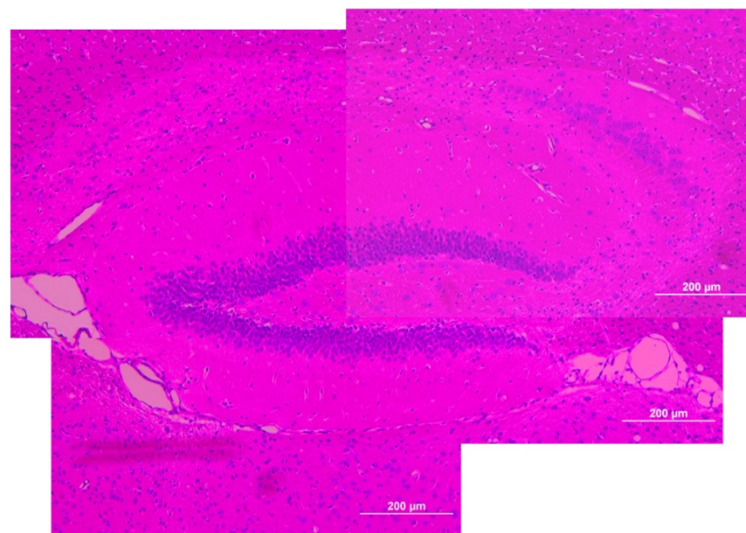


Supplemental Fig. S2



Supplemental Fig. S3

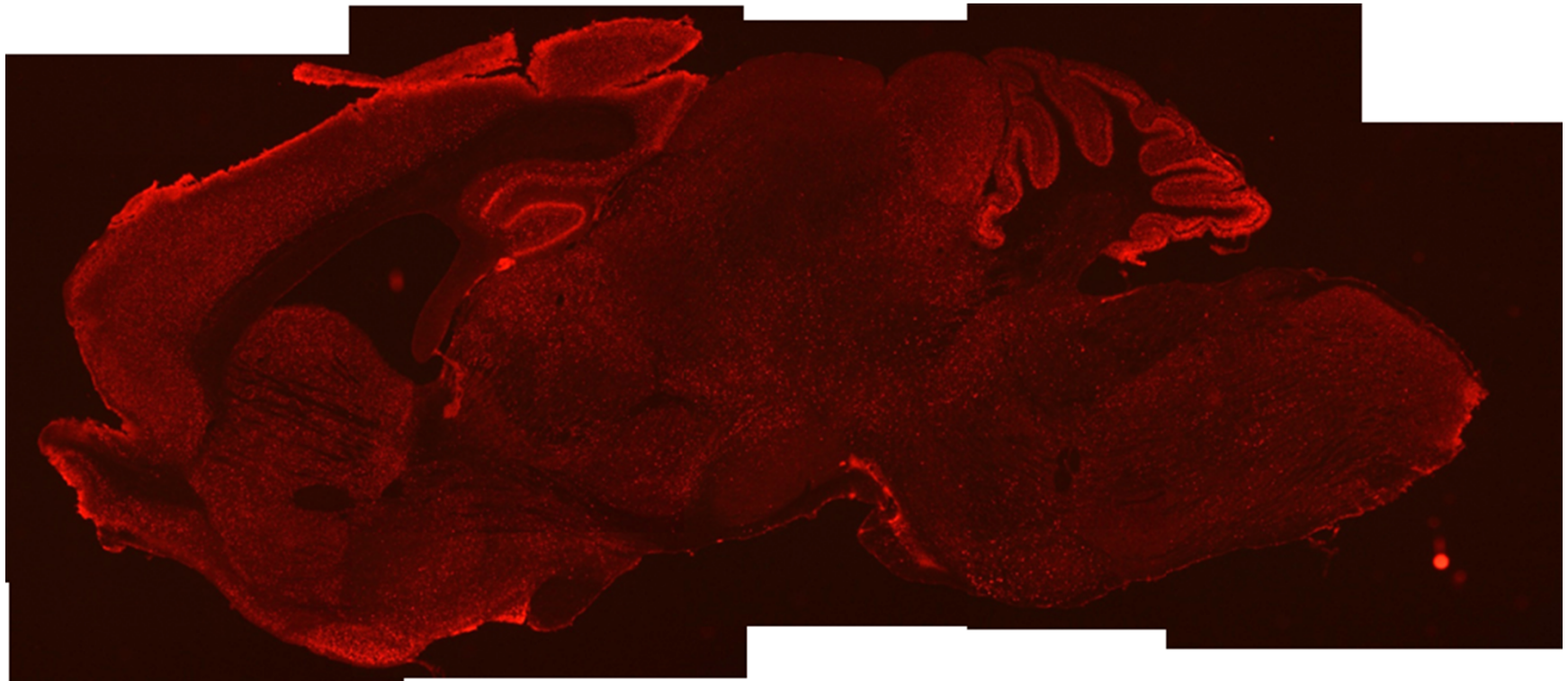
586-82Q-C63



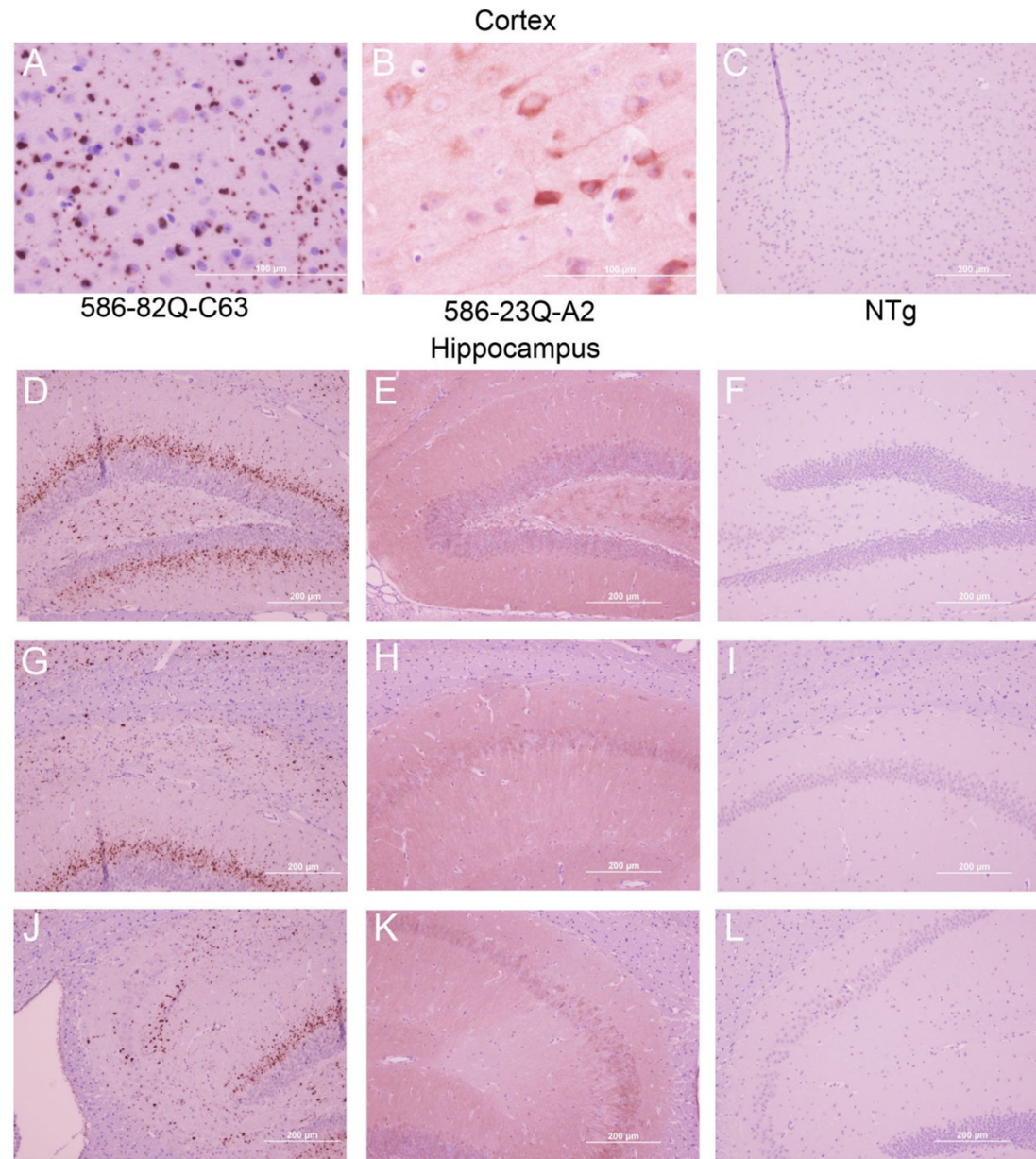
586-23Q-A2



Supplemental Fig. S4



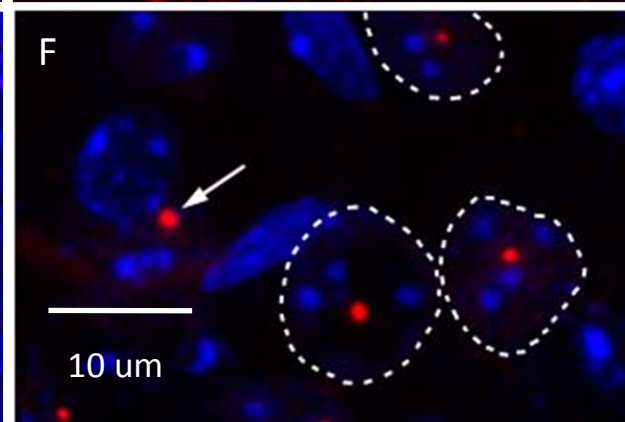
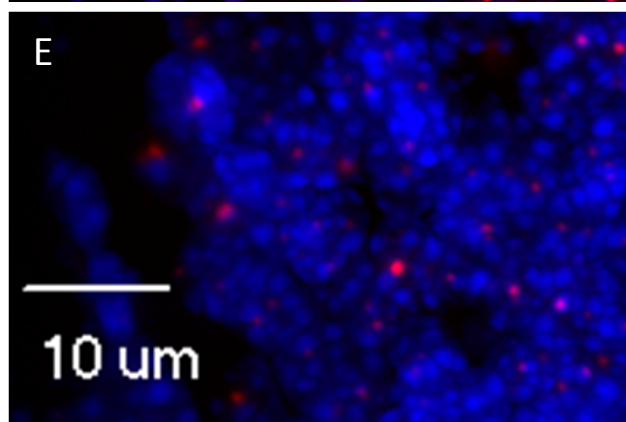
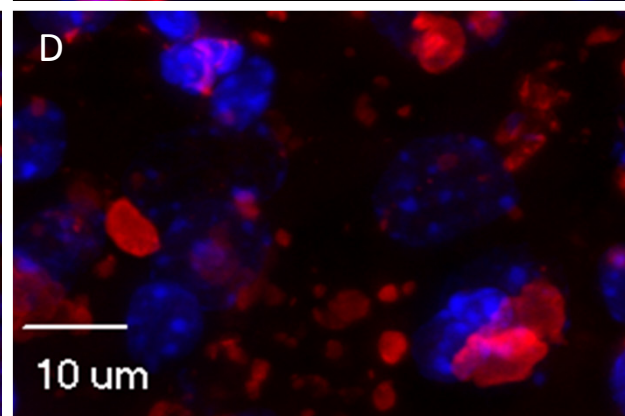
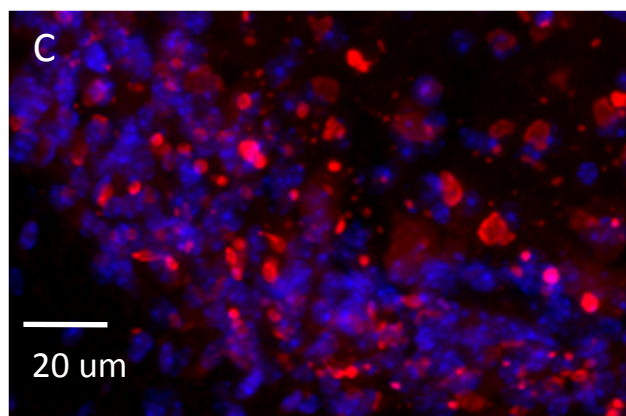
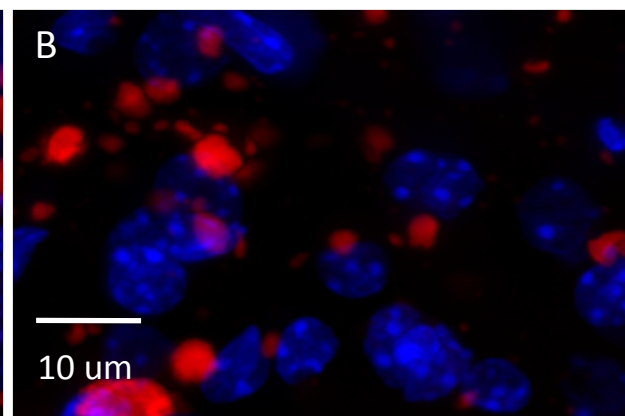
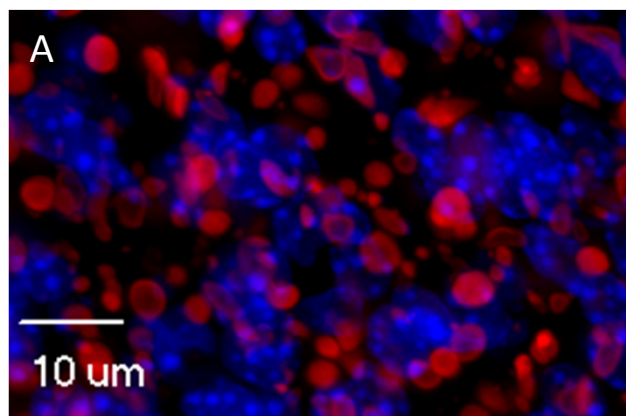
Supplemental Fig S5



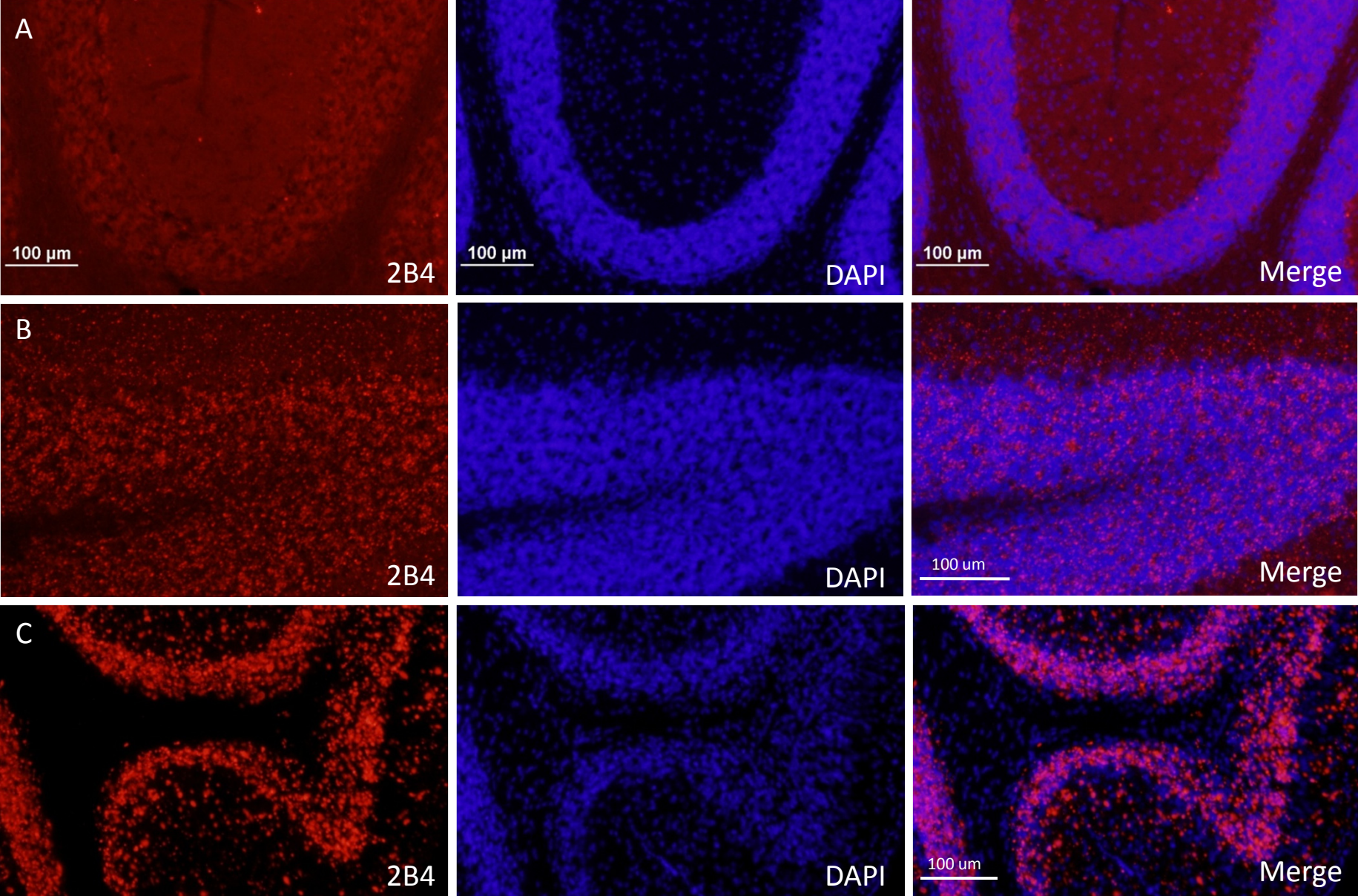
Supplemental Fig. S6

Cerebellum

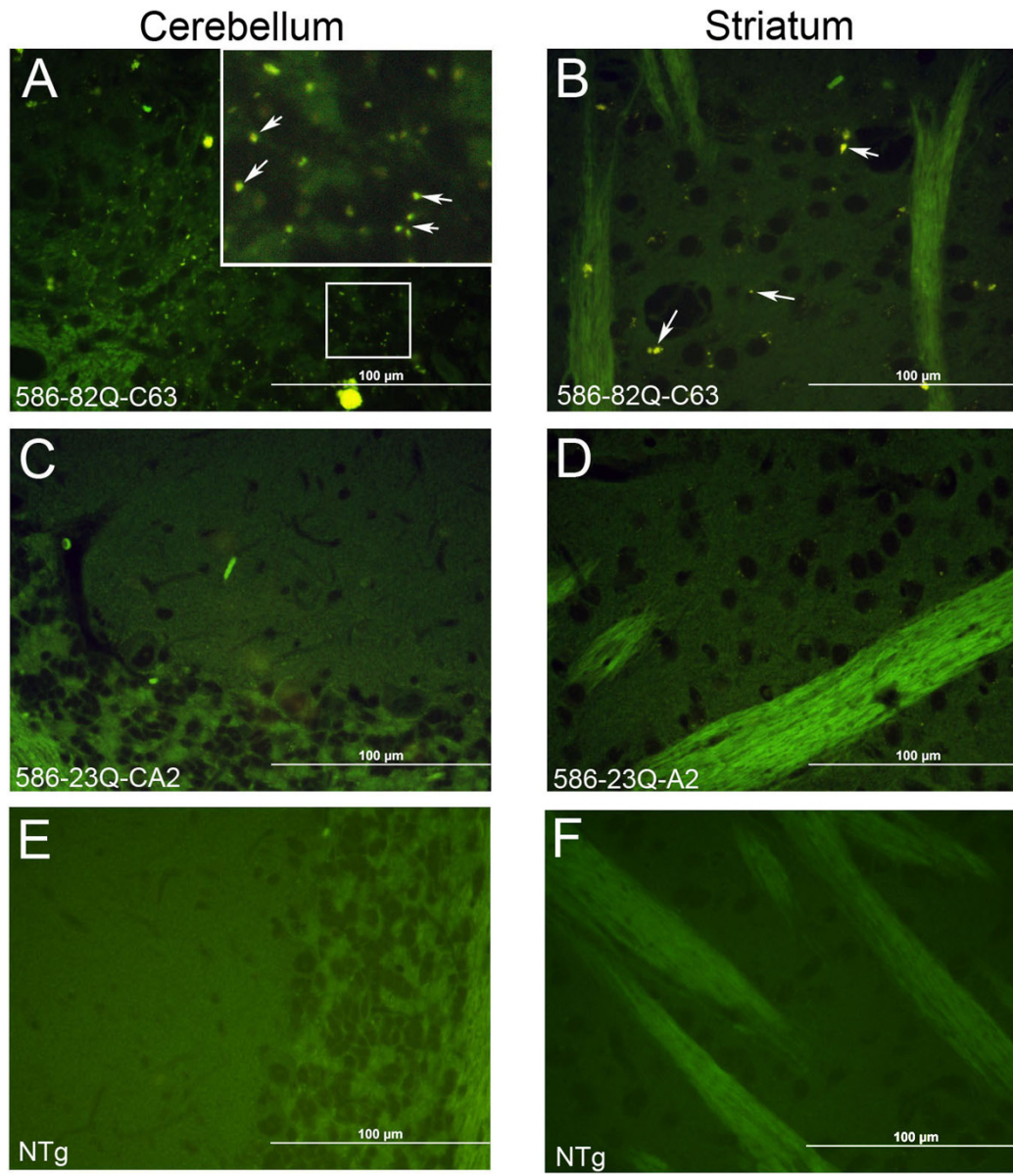
Cortex



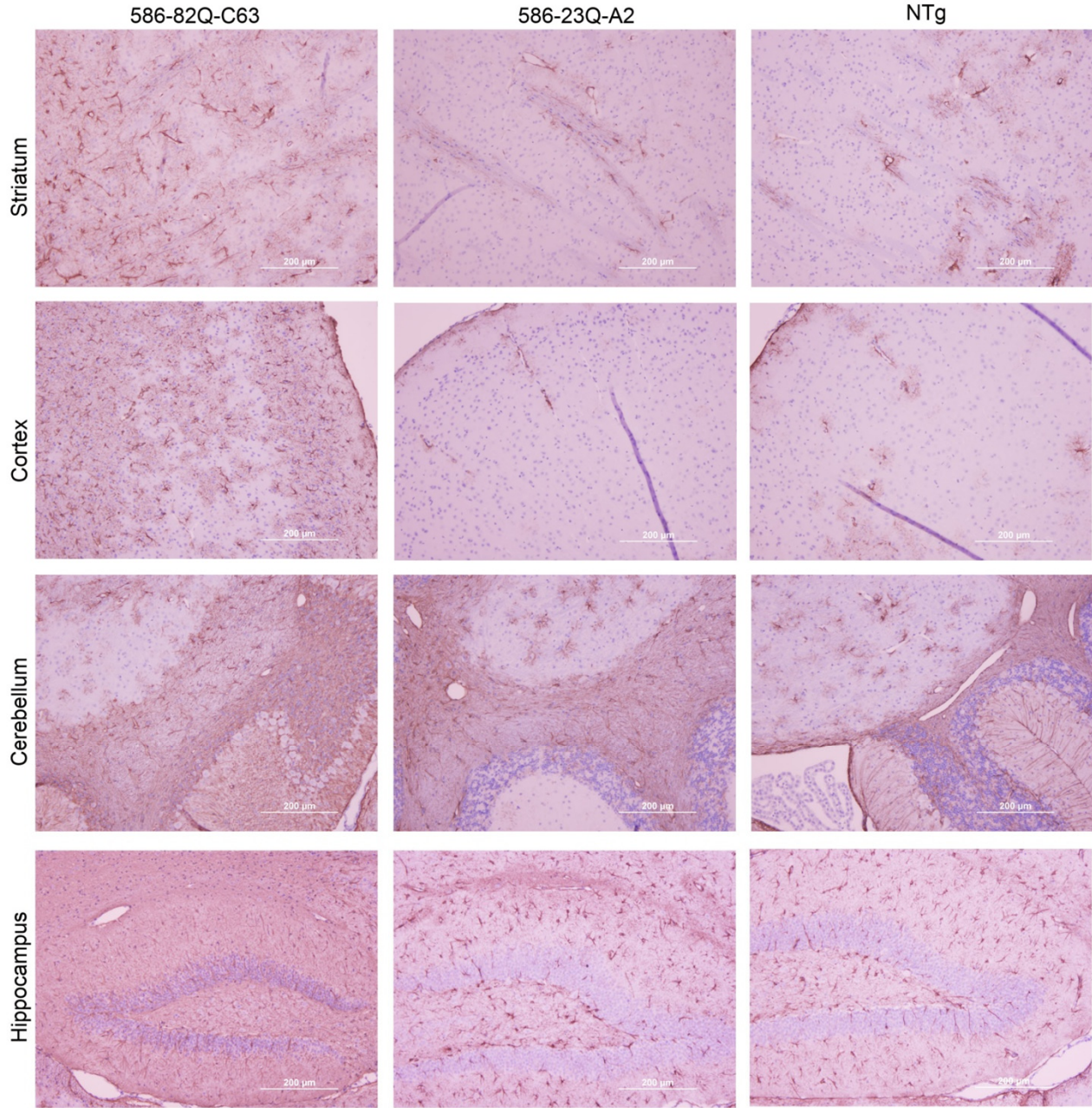
Supplemental Fig. S7



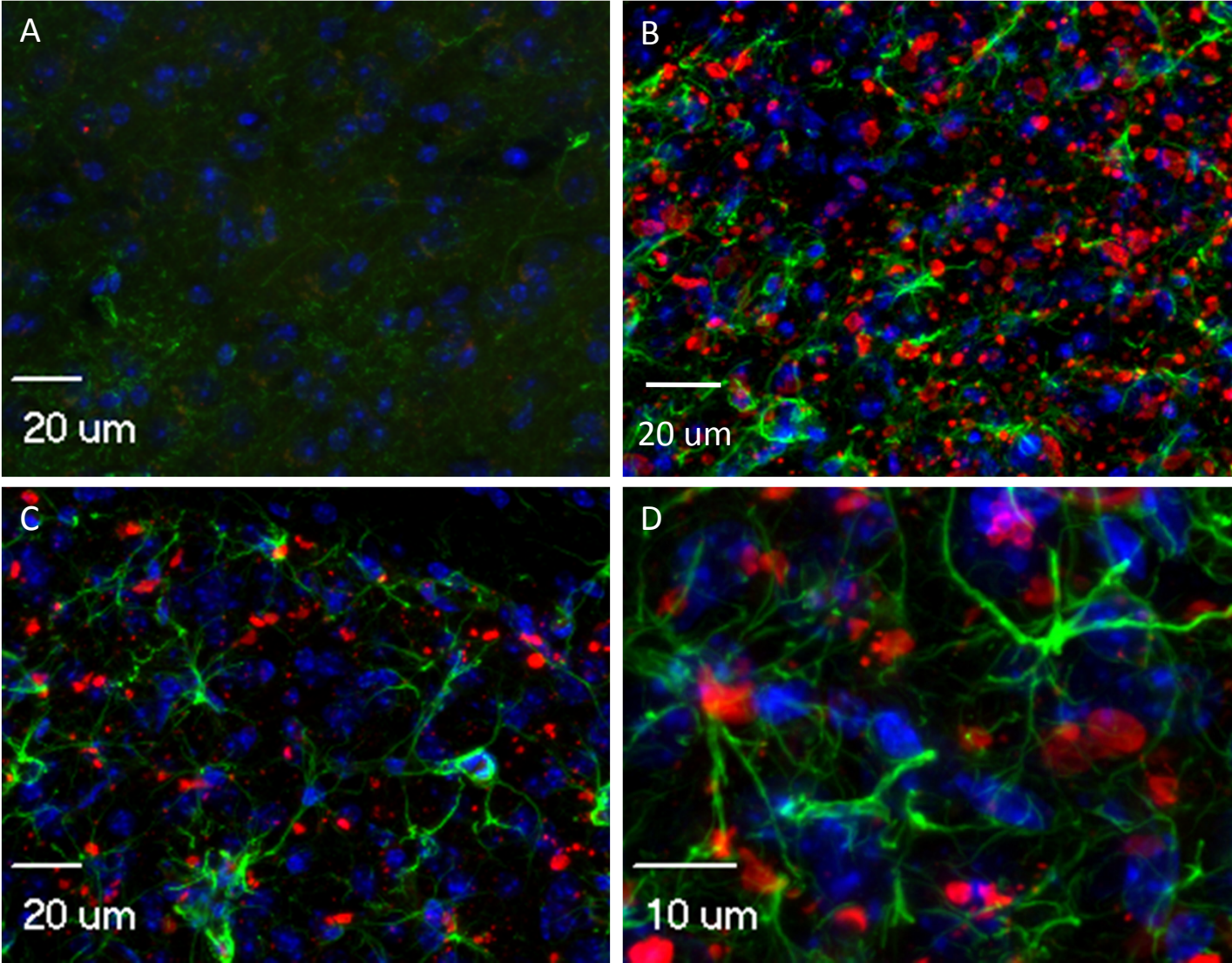
Supplemental Fig. S8



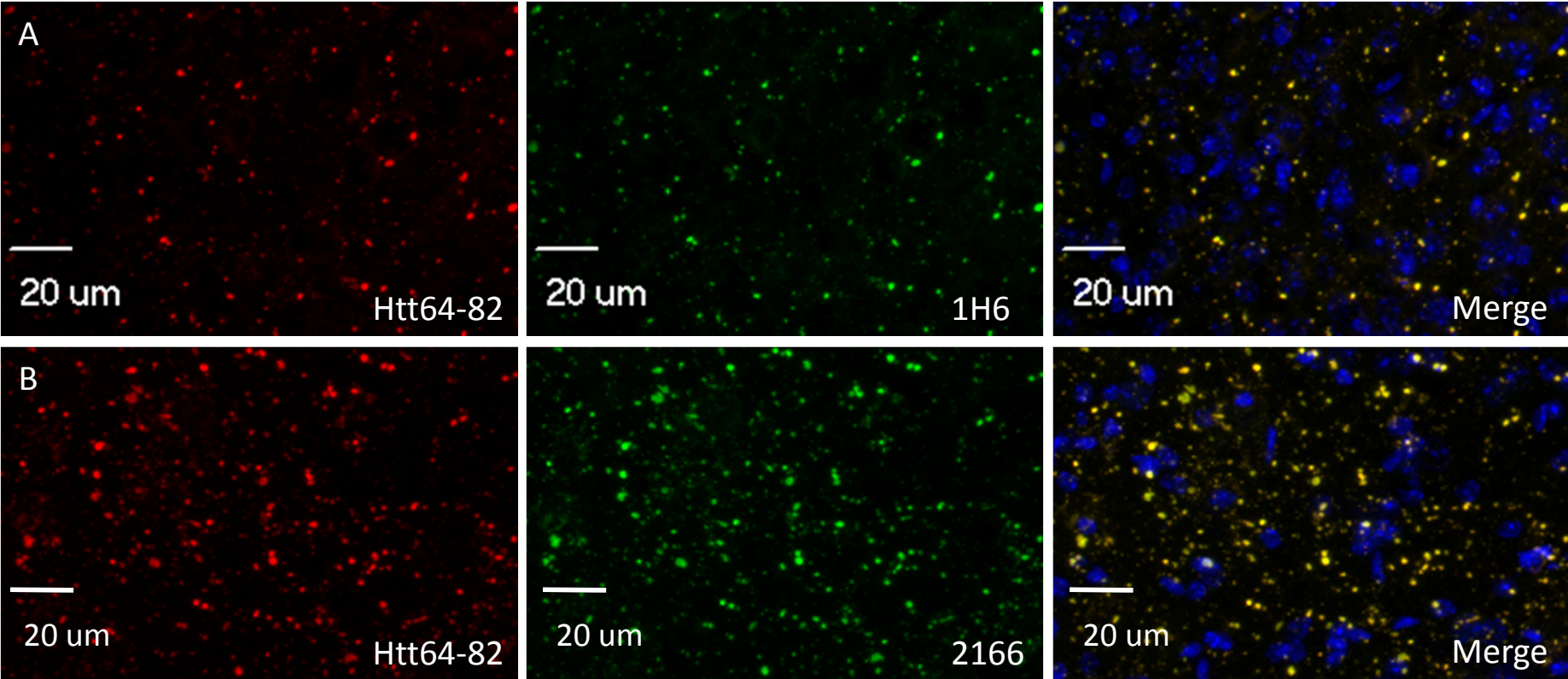
Supplemental Fig. S9



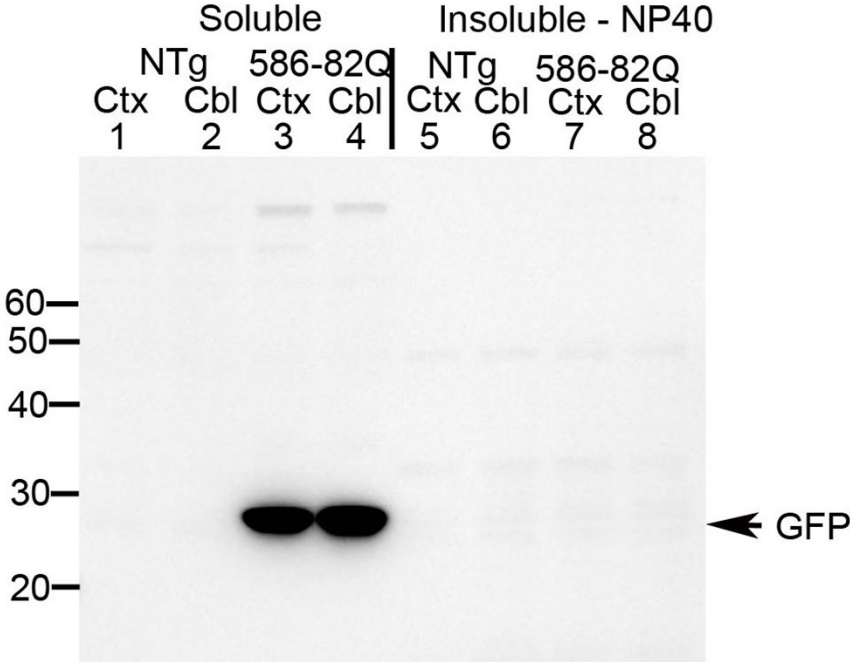
Supplemental Fig. S10



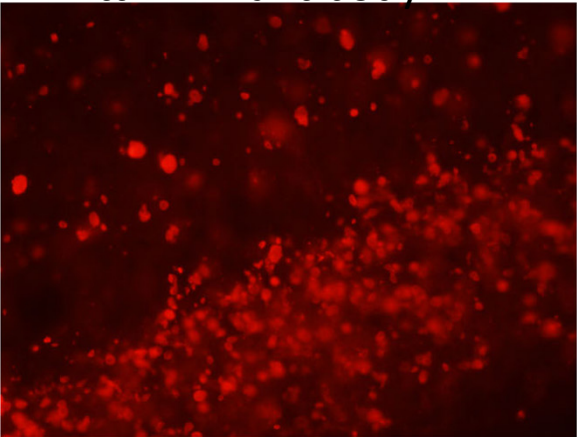
Supplemental Fig. S11



Supplemental Fig. S12



Htt -2B4 antibody



GFP

